Hwan Hwang, S., Kim, K. B., & Han, D. (2020). Comparison of methods to estimate areal means of short duration rainfalls in small catchments, using rain gauge and radar data. *Journal of Hydrology*, *588*, [125084]. https://doi.org/10.1016/j.jhydrol.2020.125084

# Comparison of methods to estimate areal means of short duration rainfalls in small catchments, using rain gauge and radar data

Seok Hwan Hwang[1], Kue Bum Kim[2*], Dawei Han[3]

[1] Department of Land, Water and Environment Research, Korea Institute of Civil Engineering and Building Technology, Goyang-si, South Korea
[2] Water resources policy division, Ministry of Environment, Sejong-si, South Korea
[3] Water and Environmental Management Research Centre, Department of Civil Engineering, University of Bristol, Bristol, UK
* Corresponding author: kbkim93@gmail.com

## Abstract

Flood forecasting for early alerts is a challenging task for hydrologists. This is particularly the case in small catchments due to a lack of upstream gauges and their flashy response. In such catchments, estimating areal mean rainfall at short intervals by applying spatial interpolation schemes based on rain gauge data in short time scales is a significant work for accurate flood forecasting. In this study, we compare and evaluate four commonly used spatial interpolation methods in small catchments, which have small numbers of rain gauges in South Korea. We investigate the impacts of catchment area on different spatial interpolation schemes. Then a simulation is done with hypothetical storms to illustrate the limitation of the Thiessen method. Local heavy rainfall events have been selected for case studies and 10-minute rain gauge rainfall data are used, since short time scales of rainfall data are generally needed for flash flood forecasting and alerts. Furthermore, we analyse the characteristics of different spatial interpolation techniques by comparing the results with weather radar rainfall. The results revealed that mean absolute percentage discrepancy (MAPD) of areal mean rainfall between the Thiessen polygon method and the other three interpolation schemes (Inverse distance weighting, Multiquadric interpolation, Kriging) increases rapidly as the catchment area becomes smaller, especially when the catchment area is less than $500km^2$. In addition, regarding the number of rain gauges in a catchment, the smaller the number of rain gauges used in calculating areal mean rainfall, the larger the MAPD becomes, as expected. Furthermore, the number of rainfall events with outliers increased as correlation among rain gauge locations increased, which implies that outliers are more likely to happen when the gauges are located in a linear format rather than in a cluster. Finally, the temporal distributions of areal mean rainfall obtained from rain gauge and weather radar data are different depending on the direction of rainfall movement, especially in sparsely gauged catchments. This study provides a possible guideline for rain gauge number and placement to estimate areal mean rainfall accurately at small catchments.



Keywords: spatial interpolation method, Thiessen polygon, Inverse distance weighting, Multiquadric interpolation, Kriging, radar rainfall

## 1. Introduction

Spatial distribution of precipitation data plays an important role in many environmental applications, especially for water resources (Chen et al., 2017; Faurès et al., 1995; Li and Heap, 2011; Ly et al., 2011; Wagner et al., 2012). Hydrologists need accurate spatial rainfall data across a catchment for hydrological risk assessment and water budget estimates. Most of the precipitation data are collected by geographically dispersed networks of rain gauges, which are point data. Rain gauges provide comparatively accurate measurement of precipitation at a point, however, they cannot fully capture the spatial variability of rainfall with time due to its temporal and spatial variability. The rain gauge data are generally used as inputs to hydrological models and the model accuracy is influenced significantly by these input data (Beven, 2011). Especially, the quality of hydrological model result depends on the quality of continuous spatial rainfall data (Andréassian et al., 2001; Kobold and Sušelj, 2005; Leander et al., 2008; Moulin et al., 2009; Singh, 1997). The use of a small number of rain gauge data may cause great uncertainties in simulated streamflow (Chaubey et al., 1999; Faurès et al., 1995), particularly when the rain gauge stations are placed outside the studied catchment (Schuurmans and Bierkens, 2006).

Various spatial interpolation schemes have been developed and applied ranging from simple methods such as Thiessen polygons (Thiessen, 1911) and Inverse Distance Weighting (IDW) (Berndt and Haberlandt, 2018; Di Piazza et al., 2011; Teegavarapu et al., 2009) to more complex methods such as Kriging which incorporate secondary information (e.g., elevation, remotely sensed observation, etc) as covariates to improve primary data. The former and the latter are also known as deterministic methods and geostatistical methods respectively (Ly et al., 2011). Conditional merging (CM) techniques have been developed which are methods of spatial interpolation suited for merging spatially continuous grid-based measurements and point measurements (Pegram, 2001; Sinclair and Pegram, 2005). The CM preserves the spatial covariance structure of spatially continuous grid-based measurements while maintaining the accuracy of the point-based measurements. Numerous comparative studies have been done to explore which spatial interpolation method for rain gauge data is the best, however there were no consistent findings (Dirks et al., 1998; Oke et al., 2009; Otieno et al., 2014; Price et al., 2000; Vicente-Serrano et al., 2003; Zimmerman et al., 1999), indicating that more studies are needed in this field. Interpolating rain gauge rainfall is a challenging task since the application of different methods may cause different results from the actual spatial distribution of rainfall, which is of course unknown.

In most studies, spatial interpolation techniques have been applied to daily, monthly and annual time steps of rainfall data (Ly et al., 2013) and only a few studies have compared interpolation methods using hourly time steps, e.g., Schiemann et al (2011). Moreover, few studies have compared interpolation schemes based at a sub-hourly time scale. Normally the spatial variability of rainfall is more obvious at shorter time scales, therefore simple spatial interpolation of rainfall may not yield an accurate measurement of the real rainfall field. This was demonstrated by Haylock et al (2008) and Yatagai et al (2009).

Recently, radar rainfall data have been used frequently as inputs for hydrological applications (Fassnacht et al., 2003; Neary et al., 2004; Tetzlaff and Uhlenbrook, 2005), especially in urban hydrology owing to the advances in technologies, numerical models, and data processing (Thorndahl et al., 2017). Unlike rain gauge data, weather radars can survey large areas and can better capture the spatial variability of rainfall fields (Ochoa-Rodriguez et al., 2019). However, they are often biased due to various factors such as topography, climate and spatio-temporal resolution (Ebert et al., 2007; Karimi and Bastiaanssen, 2015; Maggioni et al., 2016). The rain intensity is derived indirectly from the measurement of reflectivity, hence, the data is subject to systematic and random errors such as instrumental and sampling error especially in mountainous terrain (Gabella et al., 2005). In addition, radar rainfall amount is normally smaller than the rain gauge rainfall amounts (Smith et al., 2007) due to the difference in spatial domains. The typical pixel size of conventional weather radars is 1 × 1 km or 2 × 2 km whereas the sample area of a rain gauge is typically 200-300 $cm^2$.

Flood forecasting for early warning is a challenging task for hydrologists. This is particularly the case in small catchments due to a lack of upstream stream gauges and flashy rainfall-runoff response (i.e., short lead time). In such catchments, estimating areal rainfall by applying spatial interpolation schemes using rainfall data from rain gauges in short time scales (e.g. 10-minute) is valuable for accurate flood forecasting. Recently, there has been an increasing trend of localized torrential rainfall events in summer in South Korea (Boo et al., 2006; Chang and Kwon, 2007). In this context, we compare and evaluate spatial interpolation methods in small catchments which have a small number of rain gauges in South Korea. Local heavy rainfall events have been selected for case studies and 10-minute rain gauge rainfall data are used, since short time scales of rainfall data are generally needed for flash flood forecasting and alerts. Furthermore, we analyse the characteristics of different spatial interpolation techniques by comparing the results with radar rainfall.

Given this background, this paper explores the following questions:

(1) For flood forecasting, are deterministic spatial interpolation methods appropriate for small catchments with sparse rain gauge networks? If not, what are the limitations?
(2) What are the effects of rain gauge density, rain gauge distribution and rainfall direction on different spatial interpolation schemes? Are there any correlations between rain gauge density and outliers in rainfall data?
(3) Can weather radar rainfall be a useful alternative to rain gauge data at regional-scale catchments with low densities of rain gauges?

The primary objectives addressed in this paper are to: (1) assess the effects of catchment area, rain gauge density, rain gauge distribution and direction of rainfall movement on estimating areal average rainfall with different spatial interpolation methods and (2) suggest guidelines for rain gauge numbers and placement to estimate accurate areal mean rainfall on small catchments. This investigation has both practical and scientific value since it allows us to identify not only the importance of physical characteristics (i.e., number and location) of rain gauges but also the effects of rainfall movement and direction in estimating areal mean rainfall.

In Section 2, we describe the study area, rain gauge and radar rainfall data used. Spatial interpolation schemes used in this study are briefly introduced in Section 3. The impacts of catchment area, rain gauge density and rainfall direction on spatial interpolation methods are presented in Section 4. The main conclusions of this study are summarized in Section 5.

## 2. Catchment and data

### 2.1 Study area

The basins (catchments) of South Korea are classified into three groups: 21 large sized areas (Basin), 117 medium sized areas (Sub-basin) and 850 small sized areas (Standard-basin) as shown in Figure 1. Basins are divided according to the 5 largest rivers (Han River, Nakdong River, Geum River, Seomjin River, and Yeongsan River), coastal areas and Jeju Island. Each Sub-basin is divided based on the confluences of natural rivers and the major islands of the southern and western sea. Lastly, Standard-basins are divided on the basis of the point where national and regional rivers gather, the point where a dam is located and the area where major facilities that manage waters are located.

## 2.2 Precipitation data

### 2.2.1 Rain gauge data

Two sources of rain gauge data are used in this study. First, Automatic weather stations (AWS) installed by the Korea Meteorological Administration (KMA) are used. Daily rainfall data from 2001 to 2010 are used to make 5km × 5km grid rainfall. These data are used to analyse differences among spatial interpolation methods with regard to catchment area in Section 4.1. Figure 1(a) shows the distribution of 515 AWS and 117 sub-basins.

AWS installed by KMA are quite evenly distributed over South Korea. However, since AWS distribution is based on administrative district, the AWS network is weak in considering catchment characteristics. Therefore, another set of rain gauge data from the Ministry of Environment (ME), which are installed based on catchment size and used in river flood forecasting, are used instead of AWS data in Section 4.2. 10-minute rainfall data from 2016 to 2018 is used to compare the estimated areal mean rainfall difference between spatial interpolation methods when the rain gauge density changes. Figure 1(b) shows the locations of 664 standard-basins and 564 rain gauges installed by ME, which are used in river flood forecasting.

[Insert Figure 1]

### 2.2.2 Weather radar rainfall data

Weather radar data are received from 1 single polarization radar (Imjin) and 5 dual polarization radars (Biseul, Sobaek, Gari, Seodae, Mohu) operated by the Flood Control Office of ME (Ministry of Environment of Korea), which have temporal and spatial resolutions of 10-minute and 250m respectively. In this study, the Marshall and Palmer equation (Marshall and Palmer, 1948) is applied for single polarization radar quantitative precipitation estimation (QPE) and the JPOLE algorithm (Ryzhkov et al., 2005) is used for dual polarization radar QPE. The coverage and distribution of weather radars in South Korea are shown in Figure 2.

[Insert Figure 2]

## 3. Spatial interpolation schemes

We used four common interpolation techniques: Thiessen polygon, Inverse distance weighting, Multiquadric interpolation and Kriging methods. Brief introductions to the spatial interpolation schemes applied in this study are provided here, since details on various methods are available from many hydrological and statistical textbooks. In South Korea, the Thiessen polygon method is officially used for river flood forecasting, hence, differences of estimated areal mean rainfall between the Thiessen polygon method and the other three methods are compared in this study. We regenerated 495km (longitude direction) × 725km (latitude direction) grid rainfall at 5km intervals using 10-minute rainfall data. Four different interpolation schemes are applied and the areal mean precipitation is estimated by averaging the grid rainfall.

### Thiessen polygon (TSN)

The catchment area is divided into polygons with each polygon containing a rain gauge (a single point of sampling) (Chow, 1964). Each polygon represents the entire area covered by that polygon. Although this is a simple and straightforward method, it has some disadvantages. For example, the estimation is based on only a single gauge and does not incorporate the information on neighbouring points. In addition, there are sudden jumps or discontinuities across the boundaries of polygons.

**Inverse Distance Weighting (IDW)**

IDW estimates the value at an unsampled site by the distance weighted average of observed data from all sampled sites surrounding it. As the distance increases between the unknown value of the estimated point and the surrounding known sampled points, the weight decreases which means that the interpolant is less influenced by the sampled value. The weight $\lambda_i$ is calculated as

$$\lambda_i = \frac{D_{0i}^{-d}}{\sum_{j=1}^{n} D_{0j}^{-d}}$$

where $D_{0i}$ is the distance from the sampled point to the estimated point, *d* is the geometric form of the weight, *n* is the number of known value locations. The power *d* was set to 2, which was found not to be significantly different from the results realized by optimal power values (Otieno et al., 2014).

**Multiquadric Interpolation (MQI)**

The MQI was first developed by Hardy (Hardy, 1971) for the interpolation of irregular surfaces in geophysical sciences. Then it was applied to rainfall surfaces with the satisfactory result for determining areal rainfall (Shaw and Lynn, 1972). Multiquadric analysis represents the surface to be approximated as a summation of a number of individual quadric surfaces. The catchment perimeter is determined by a polygon of *m* sides whose vertices are given by the pairs $(x_k, y_k)$, $k=1,2,\ldots,m$. Inside and outside this polygon are *n* rain gauges whose coordinates are $(g_i, h_i)$, $i=1,2,\ldots,n$. A rainfall amount is recorded at each rain gauge, and the amount is given as $z_i$. Multiquadric hyperboloids centered at each rain gauge take the following form:

$$z_i = \sum_{j=1}^{n} \left[(g_j - g_i)^2 + (h_j - h_i)^2 + a^2\right]^{1/2} c_j$$

A number of researchers have used MQI (e.g. Pegram and Pegram, 1993) and readers are referred to the papers cited above for the details about this method.

### Kriging (KRG)

In this study Ordinary Kriging (Wackernagel et al., 1997) is used which is the standard version of Kriging. KRG is categorized as a univariate approach since no additional information is considered except for one data source. The KRG estimate at a point $u_0$ is calculated as follows:

$$Z^*(u_0) = \sum_{1}^{n} \lambda_i Z(u_i)$$

where, $\lambda_i$ is the weight of each of the $n$ adjacent observations taken into account. The weights are obtained by solving the kriging system:

$$\sum_{j=1}^{n} \lambda_j \gamma\left(u_i - u_j\right) + \mu = \lambda\gamma(u_i - u_0) \; for\ i=1,\ \ldots\ ,n, \qquad \sum_{j=1}^{n} \lambda_j = 1$$

here, $\mu$ is a Lagrange multiplier. Kriging requires a variogram model to estimate its weights. In this study, the least squares method has been applied due to its computational simplicity and broad availability. The least squares variogram parameter estimates are those that minimize the squared differences between the experimental variogram and theoretical model. In this study, the spherical model was adopted to perform a least squares fit of theoretical variograms to an experimental variogram. In order to perform semivariogram analysis and subsequent KRG, GSTAT software (Pebesma and Wesseling, 1998) was used. The estimated correlation distance varies depending on the regions and events. In this study, it was set in the range of 20 to 40 km.

## 4. Results and discussion

The first part of this section investigates the impacts of catchment area on different spatial interpolation schemes. Then a simulation is done with hypothetical storms to illustrate the limitation of TSN by presenting the effects of rain gauge distribution and storm direction on estimated areal mean rainfall when TSN is applied at small catchments. Finally, effects of rain gauge density, distribution and the direction of rainfall movement on spatial interpolation methods are explored with real recorded rainfall data at small catchments.

### 4.1 Effects of catchment area on spatial interpolation schemes

Areal mean annual rainfall (AMAR) in Mid-Sized catchments over South Korea is studied to explore the impact of catchment area on different spatial interpolation schemes. Mean absolute percentage discrepancy (MAPD) has been estimated with Equations (1) to (3) to compare against the TSN method. Among 117 Mid-Sized catchments in South Korea, the following types of catchments (66 Mid-Sized catchments) are excluded for consistent comparison: catchments that contain no rain gauges, catchments near the Demilitarized Zone, catchments near the complex coastline and catchments where mean elevation is higher than 400m.

$$MAPD_{IDW} = \frac{|AMAR_{TSN} - AMAR_{IDW}|}{AMAR_{TSN}} \times 100 \tag{1}$$

$$MAPD_{KRG} = \frac{|AMAR_{TSN} - AMAR_{KRG}|}{AMAR_{TSN}} \times 100 \tag{2}$$

$$MAPD_{MQI} = \frac{|AMAR_{TSN} - AMAR_{MQI}|}{AMAR_{TSN}} \times 100 \tag{3}$$

where, $AMAR_{TSN}$, $AMAR_{IDW}$, $AMAR_{KRG}$, $AMAR_{MQI}$ are areal mean annual rainfall obtained from TSN, IDW, KRG and MQI respectively. Figure 3 presents mean absolute percentage discrepancy (MAPD) of areal mean annual rainfall for different spatial interpolation schemes and catchment area. As shown in Figure 3, MAPD and catchment area are inversely proportional. In addition, the MAPD between TSN and the other three interpolation schemes increase rapidly as the catchment area becomes smaller, especially when the catchment area is less than $500km^2$ (shaded pink in the figure). This might be because normally small catchments in South Korea have complicated topography and low density of rain gauges. In the case of large catchments, differences tend to be less than 2% and almost constant, which means that there are no obvious distinctions among the four interpolation techniques.

[Insert Figure 3]

Since the differences between the four spatial interpolation schemes are large in catchments smaller than $500km^2$, the drawbacks of applying different interpolation methods at small catchments are analysed in the next section by illustrating a conceptual simulation for an example and presenting the result of real cases.

## 4.2 Limitation of the spatial interpolation scheme on small catchments

### 4.2.1 Effects of rain gauge distribution and rainfall direction on TSN

The flaw of TSN is demonstrated as an example in Figure 4. Let us assume that the four rain gauges (A, B, C and D) are all located outside the catchment and the storm is moving, i.e. the rainfall direction is from South West to North East (Case 1) and vice versa (Case 2). In Case 1, although the rainfall pass through the catchment, the areal rainfall of the white hatched part of the catchment may not be estimated until the storm arrives at Rain Gauge A, which is placed outside the catchment. As a result, in this case, peak rainfall will be estimated later than the real peak rainfall. On the other hand, in Case 2, when the storm arrives at Rain Gauge A, areal rainfall of the white hatched part of the catchment is computed even though the rainfall has not arrived at the catchment yet. Consequently, in this case, peak rainfall will be estimated beforehand rather than when the real peak rainfall occurs.

[Insert Figure 4]

As explained in the previous paragraph, TSN has structural limitations in estimating areal mean precipitation. The following hypothetical example in Figure 5 also demonstrates the drawback of using TSN in calculating areal mean precipitation. The experimental set up for this example is as follows:

- The unit of time and distance is ignored since this is a hypothetical example.
- The horizontal axis indicates the movement of rainfall and the vertical axis is the time scale.
- A spatial distribution pattern of the hypothetical rainfall is modeled in five horizontal grids, the intensity of each grid having 5, 7, 10, 13 and the 7mm respectively. The storm is moving from left to right with constant velocity, two grids at each time step.

- The distances between rain gauges are set further apart than the size of the storm (five grids) since the study case in this study is a small catchment with a low density of rain gauges.
- The region is divided into three sub-regions. On the horizontal axis, three hypothetical rain gauges (green vertical bars) (A, B, C) are in a line. The area of each sub-region is assumed to be the number of grid squares that each sub-region has. In this case, the area is 16, 11 and 18 for polygon A, B, and C respectively, as indicated by the red captions at the bottom of the figure.
- Since the total catchment area is 45, the areal proportion of each sub-region A, B and C is 0.36, 0.24 and 0.40 respectively.

Under these conditions, while the rainfall moves from left to right it will pass through rain gauge A, B and C in order and the areal mean rainfall will be estimated by the ratio of sub-region weight. Since the shape of storm and rainfall intensity remains unchanged, true areal mean rainfall should be constant regardless of time. However, when TSN is applied, since the distance between the rain gauges is larger than the size of the rainfall (5 grid squares), the areal rainfall of each sub-region is estimated only when the rainfall arrives at the gauge. Therefore, although the true areal mean rainfall is constant (GRD), the estimated areal mean rainfall is fluctuating sharply in a serrated shape (TSN) as shown in the right panel of Figure 5. For instance, when the center of the moving rainfall (i.e., the maximum value in this rainfall) just arrives on the rain gauge, areal mean rainfall may be overestimated with the value close to the point rainfall. On the other hand, if the rainfall is away from the rain gauge areal mean rainfall may be underestimated with the value of zero. As shown in this demonstration, TSN has structural limitations in computing areal mean rainfall, and therefore the amount of estimated areal mean rainfall might be distorted especially when the catchment is small and the rain gauge density is low.

[Insert Figure 5]

**4.2.2 Effects of rain gauge density and Interpolation method**

To demonstrate the effects of rain gauge density on estimated areal mean rainfall with different spatial interpolation methods applied, rainfall events in each of 664 Standard-basins between the year 2016 and 2018 were selected and analysed. Six hundred and sixty four Standard basins were chosen from among all 850 Standard-basins, since they are used for flood forecasting in South Korea. Rainfall events that meet the following two conditions in each Standard-basin are considered as outliers and have been excluded: (1) cumulative areal mean rainfall using radar rainfall data is less than 10mm; (2) estimated areal mean rainfall difference between using rain gauge data and radar rainfall data is larger than a factor of three. Finally, 528 Standard-basins and 1404 rainfall events were chosen for areal mean rainfall analysis in this study. Figure 6 shows the distribution of catchment area over the 528 standard-basins.

[Insert Figure 6]

Figure 7 shows how areal mean rainfall was modelled. To evaluate the effects of rain gauge density on areal mean rainfall calculated from four different interpolation methods, reference areal mean rainfall is needed. In this study areal mean rainfall estimated using radar rainfall data is set as a reference since radars can survey large areas and can better capture the spatial variability of rainfall fields (Ochoa-Rodriguez et al., 2019). Here, the bias of radar data was not adjusted by rain gauges for the following reasons: (1) the key process of correcting the bias of radar includes matching underlying statistical properties between the radar and rain gauge data. Therefore, the result of comparing different spatial interpolation methods may be distorted by a bias adjustment process, (2) adjusting radar rainfall estimates by rain gauge observations may not remove the bias entirely. Rainfall data is collected from rain gauges, and the corresponding radar rainfall estimate is taken from the radar grids, at a very large difference of scale, which is used to calculate areal mean rainfall. The mean absolute percentage error (MAPE) is commonly used in model evaluation, due to its intuitive interpretation in terms of relative error. Therefore, MAPE of four different interpolation methods is estimated as in Equation 4.

$$MAPE_{ITP}^{RDR} = \frac{|AMR_{GRD}^{RDR} - AMR_{ITP}^{RDR}|}{AMR_{GRD}^{RDR}} \times 100 \qquad (4)$$

where, the superscript RDR represents radar and ITP represents interpolation methods. TSN, IDW, KRG and MQI. $AMR_{ITP}^{RDR}$ are areal mean rainfall estimates obtained from radar grids at corresponding rain gauge points using *TSN*, *IDW*, *KRG* and *MQI* interpolation methods respectively. $AMR_{GRD}^{RDR}$ is areal mean rainfall estimated from radar grid rainfall.

[Insert Figure 7]

Figure 8 shows the MAPE with regard to the number of gauges used in estimating areal mean rainfall. The box height represents the 25$^{th}$ percentile (1$^{st}$ quartile) to the 75$^{th}$ percentile (3$^{rd}$ quartile) of MAPE sets, which is generally called as interquartile range (IQR). The mid horizontal line that goes through each box represents the median and the black circle represents the mean value. The whiskers are the two lines outside the box that extend to the highest and lowest value ($1.5 \times$ IQR). The range of IQR and 1.5 IQR of IDW and KRG is less than those of MQI and TSN when the number of rain gauge is less than two. However, when the number of rain gauge is more than three, the differences among the four methods are not large. An interesting thing is that, for MQI, when the rain gauge number is less than two, the range of IQR is the widest and the mean value is the largest, while the median value is not that different from the other methods. This indicates that there are some big storm events that affect MAPE and the mean value when MQI is applied, but in general, MAPE is not that large compared with the other three methods.

[Insert Figure 8]

Analogous to other studies (Bárdossy and Pegram, 2013; Borga and Vizzaccaro, 1997), the performance of the interpolation methods is dependent on the rain gauge density. As can be seen in Figure 9, areal mean rainfall differences between the interpolation methods decrease as the number of rain gauges increase. The red line with circular dots in Figure 9 shows the best fit line (the second degree polynomial equation) of the mean value of MAPE. MAPE shows 20% when a single rain gauge is used in estimating areal mean rainfall. The MAPE decreases by about 10% as the number of gauges increase until 5, then decrease by about 5% as the number of gauges increase until 8. In addition, more than 8 rain gauges in Standard-basins make the effect of the number of rain gauges small in estimating areal mean precipitation.

[Insert Figure 9]

The mean percentage error (MPE) is estimated as in Equation 5 and the results are presented in Figures 10 and 11:

$$MPE_{ITP}^{RDR} = \frac{AMAR_{GRD}^{RDR} - AMAR_{ITP}^{RDR}}{AMAR_{GRD}^{RDR}} \times 100 \qquad (5)$$

In common with MAPE results, as the number of rain gauges used in calculating areal mean annual rainfall increases, the MPE between areal mean annual rainfall estimated from radar grid rainfall and four interpolation methods decreases. However, unlike MAPE, MPE shows a clear trend according to the number of rain gauges. IDW tends to underestimate (maximum mean 6.0%), while TSN tends to overestimate (maximum mean 11.9%). KRG and MQI tend to overestimate a little when less than two rain gauges are used, but when more than two rain gauges are used there is no clear bias trend overall. Figure 11 illustrates the mean value of MPE extracted from Figure 10. Among 528 standard-basins, the proportion of the basins that have rain gauges less than or equal to 4 per standard-basin are 70.5% and the rain gauges less than or equal to 6 per standard basins are 94.9%. This indicates that, for example, when the TSN method is used, the error of the estimated areal rainfall is about 5% in about 70% of standard-basins, and the error of the estimated areal rainfall is about 3% in about 95% of standard-basins.

[Insert Figure 10]

[Insert Figure 11]

#### 4.2.3 Effects of rain gauge distribution

It is evident from Figure 8 that MAPE decreases as the number of rain gauge used in calculating areal mean rainfall increases. However, the mean value of MAPE (circle marks in Figure 8) appears irregularly at similar numbers of rain gauges. From this, it can be assumed that there might be some other factors than the density of rain gauges that affect areal mean rainfall estimation. Since the shape of catchments and locations of rain gauges are fixed, it is reasonable to assume that this might be attributed to characteristics of rainfall that vary. Although catchment shape and the number of rain gauges used are similar as illustrated in Figure 6, areal mean rainfall could be substantially different due to the placement of rain gauges. The reason is that the weight of each rain gauge differs according to the shape and movement of the areal distribution of rainfall. Moreover, as discussed in section 4.2.1, interpolation methods based on rain gauges such as TSN, areal mean rainfall could be overestimated due to a specific rain gauge rainfall if the density of rain gauge is low (i.e. rain gauges are far apart compared with cloud width) and the rainfall area is located over a particular rain gauge. On the other hand, in an area where there are no rain gauges, its area mean rainfall is likely to be poorly estimated. As a result, over- and underestimation of rainfall results, so that outliers occur repeatedly.

To summarize, in this section, we examined the effects of rain gauge distribution patterns on estimated areal mean rainfall. In other words, the number of rainfall events that include outliers (i.e. extremely over- and under estimated values) are examined for different distributions of rain gauges. The linearity of a rain gauge distribution is measured by Spearman's correlation coefficient between the locations (i.e. latitude and longitude) of rain gauges. Figure 12 represents a schematic of the rain gauge distribution. When rain gauges are radially distributed as Figure 12(a), linear correlation coefficient among gauge locations is small, while in the case that rain gauges are linearly distributed as Figure 12(b), the linear correlation coefficient among gauge locations is large but, in the end, it is a function of interstation distance between them.

[Insert Figure 12]

To investigate whether or not outliers occur depending on the distribution of rain gauges, the relationship between frequency of outlier occurrence and rain gauge locations was estimated. An outlier is defined based on the so-called 'three sigma rule of thumb', i.e. estimated areal mean rainfall that lie within three standard deviations about the mean value are assumed as outliers. Sixty-one rainfall events at 664 Standard-basins, which are used in flood forecasting, were analysed.

In Figure 13, the green bar graph shows the number of rainfall events that include outliers (left y-axis) according to the correlation coefficients of the geometric distribution of gauges (x-axis) in the Standard-basin. The solid red lines represent the empirical cumulative distribution function (ECDF, right y-axis) of this bar graph series, and the pink dotted line represents 95% confidence interval of ECDF. The number of rainfall events with outliers increases as the correlation among rain gauge locations increases. This implies that outliers are more likely to happen when the gauges are located in a linear format. Especially, the slope of outlier occurrence changes from 0.83 to 1.44 before and after when the correlation coefficient is 0.7, which means that the stronger the linearity of rain gauge distribution is, the bigger the tendency of the frequency of outliers' occurrence grows. Therefore, as expected, not only the rain gauge density but also the distribution of rain gauges influences the accuracy of areal mean rainfall estimation. In addition, the reason for the difference of MAPE between similar numbers of rain gauges in Figure 8 might be due to the problem of rain gauge distribution. This implies that the shape and distribution of rain gauges is important in order not to over- or underestimate areal mean rainfall at small catchments, as expected.

[Insert Figure 13]

#### 4.2.4 Effects of rainfall direction

The distribution of rain gauges and movement of rainfall events not only affect the magnitude of areal mean rainfall but also the temporal distribution of areal mean rainfall. To investigate this, the occurrence time of peak rainfall was compared between time series of rain gauge based areal mean rainfall and radar based areal mean rainfall, at 10 minute intervals. Figure 14 shows an example of the time lag of peak rainfall occurrence depending on rain gauge placement and rainfall movement. The rain gauge is located outside the catchment on the bottom right of the 4 colored maps (black circle) in this Standard-basin (102307). The white arrows indicate the direction of rain storm. The storm happened between 00:00 (AM) to 12:00 (AM) on May 16, 2018. In the beginning of the rainfall event (time $t$ and $t+1$), the storm is moving from right to left. Therefore, the peak areal mean rainfall from rain gauge ($G^t$,$G^{t+1}$) is estimated earlier than from radar data ($R^t$, $R^{t+1}$). However, at the end of the rainfall event (time $t'$ and $t'$+1), storm is moving from left to right. Therefore, the peak areal mean rainfall from radar data ($R^{t'}, R^{t'+1}$) is estimated earlier than from rain gauge ($G^{t'}, G^{t'+1}$). In this case, the point rainfall is the same as the areal mean rainfall since only one rain gauge is located outside the catchment. Therefore, when the center of the storm passes the rain gauge, areal mean rainfall might be overestimated. This result could be another reason for irregular MAPE in Figure 8 among a similar number of rain gauges. It can be concluded from this result that in order to calculate accurate areal mean rainfall from gauges, not only the number of rain gauges but the isotropic and uniform placement of rain gauges is important.

[Insert Figure 14]

## 5. Conclusions

The main objective of this study was to assess the influence of catchment area, rain gauge density, rain gauge distribution and direction of rainfall movement on estimating areal mean rainfall, by comparing the result of four different spatial interpolation methods. The main results and conclusions can be summarized as follows:

(1) MAPD (mean absolute percentage discrepancy) and catchment area are inversely proportional. In addition, MAPD between TSN (Thiessen polygons) and the other three interpolation schemes increase rapidly as catchment area becomes smaller when the catchment area is less than $500km^2$.

(2) Regarding the influence of rain gauge density (i.e. the number of rain gauges in the catchment), the fewer the number of rain gauges used in calculating areal mean rainfall are, the larger the MAPD becomes. In our study, MAPD has a value of 20% when only one rain gauge is used in estimating areal mean rainfall. MAPD decreases to about 10% as the number of rain gauges increase to 5, then decreases to about 5% as the number of rain gauges increase to 8. In addition, more than 8 rain gauges per basin will only improve the estimation of mean annual precipitation discrepancy below 5%, which will be impractical.

(3) The IDW method tends to underestimate areal mean rainfall while TSN tends to overestimate and is spatially biased in relatively sparse networks. Therefore, KRG and MQI are recommended in estimating areal mean rainfall on small catchments.

(4) The number of rainfall events with outliers increases as the correlation among rain gauge locations (linearity of rain gauge distribution) increases. Especially, outliers increase steeply when correlation coefficients are over 0.7. This implies that outliers are more likely to happen when the gauges are located in a linear pattern. Therefore, considerations of spatial distribution of rain gauges is important in order not to over- or underestimate areal mean rainfall.

(5) Depending on the direction of rainfall movement, temporal distributions of areal mean rainfall are different when comparing rain gauge and weather radar data, especially when catchments have sparse rain gauges if Thiessen polygons are used as interpolants.

In South Korea, the Thiessen polygon method, which is out-dated, is officially used for river flood forecasting. This study clearly demonstrates that there are practical limitations in estimating areal mean rainfall when rain gauge rainfall data is obtained from small catchments. A possible solution of limitations in estimating areal mean rainfall could be merging radar and gauge data. Neither of them is accurate, but the combination is better than working with only the one or the other (Pegram, 2001; Sinclair and Pegram, 2005). In addition, differences in areal mean rainfall have been presented when different interpolation methods are applied, which can provide guidelines for which interpolation method should be selected for different conditions and how the rain gauges should be distributed to improve the accuracy of areal mean rainfall estimates.

## Appendix I. List of Acronyms

| | |
|---|---|
| AWS | Automatic weather stations |
| AMAR | Areal mean annual rainfall |
| IDW | Inverse distance weighting |
| IQR | Interquartile range |
| KMA | Korea Meteorological Administration |
| KRG | Kriging |
| MAPD | Mean absolute percentage discrepancy |
| MAPE | Mean absolute percentage error |
| ME | Ministry of Environment |
| MPE | Mean percentage error |
| MQI | Multiquadric interpolation |
| QPE | Quantitative precipitation estimation |
| TSN | Thiessen polygon |

## References

.

Andréassian, V., Perrin, C., Michel, C., Usart-Sanchez, I., Lavabre, J., 2001. Impact of imperfect rainfall knowledge on the efficiency and the parameters of watershed models. Journal of Hydrology, 250(1-4): 206-223.

Bárdossy, A., Pegram, G., 2013. Interpolation of precipitation under topographic influence at different time scales. Water Resources Research, 49(8): 4545-4565.

Berndt, C., Haberlandt, U., 2018. Spatial interpolation of climate variables in Northern Germany—Influence of temporal resolution and network density. Journal of Hydrology: Regional Studies, 15: 184-202.

Beven, K.J., 2011. Rainfall-runoff modelling: the primer. John Wiley & Sons.

Boo, K.O., Kwon, W.T., Baek, H.J., 2006. Change of extreme events of temperature and precipitation over Korea using regional projection of future climate change. Geophysical Research Letters, 33(1).

Borga, M., Vizzaccaro, A., 1997. On the interpolation of hydrologic variables: formal equivalence of multiquadratic surface fitting and kriging. Journal of Hydrology, 195(1-4): 160-171.

Chang, H., Kwon, W.-T., 2007. Spatial variations of summer precipitation trends in South Korea, 1973–2005. Environmental Research Letters, 2(4): 045012.

Chaubey, I., Haan, C., Salisbury, J., Grunwald, S., 1999. QUANTIFYING MODEL OUTPUT UNCERTAINTY DUE TO SPATIAL VARIABILITY OF RAINFALL 1. JAWRA Journal of the American Water Resources Association, 35(5): 1113-1123.

Chen ,Tao, Liliang Ren, Fei Yuan, Xiaoli Yang, Shanhu Jiang, Tiantian Tang, Yi Liu, Chongxu Zhao and Liming Zhang, 2017. Comparison of spatial interpolation schemes for rainfall data and application in hydrological modeling. Water, 9(5): 342.

Chow, V.T., 1964. Handbook of applied hydrology.

Di Piazza, A., Conti, F.L., Noto, L.V., Viola, F., La Loggia, G., 2011. Comparative analysis of different techniques for spatial interpolation of rainfall data to create a serially complete monthly time series of precipitation for Sicily, Italy. International Journal of Applied Earth Observation and Geoinformation, 13(3): 396-408.

Dirks, K., Hay, J., Stow, C., Harris, D., 1998. High-resolution studies of rainfall on Norfolk Island: Part II: Interpolation of rainfall data. Journal of Hydrology, 208(3-4): 187-193.

Ebert, E.E., Janowiak, J.E., Kidd, C., 2007. Comparison of near-real-time precipitation estimates from satellite observations and numerical models. Bulletin of the American Meteorological Society, 88(1): 47-64.

Fassnacht, S., Soulis, E., Kouwen, N., 2003. Radar precipitation for winter hydrological modelling. International Association of Hydrological Sciences, Publication(282): 35-42.

Faurès, J.-M., Goodrich, D., Woolhiser, D.A., Sorooshian, S., 1995. Impact of small-scale spatial rainfall variability on runoff modeling. Journal of hydrology, 173(1-4): 309-326.

Gabella, M., Bolliger, M., Germann, U., Perona, G., 2005. Large sample evaluation of cumulative rainfall amounts in the Alps using a network of three radars. Atmospheric research, 77(1-4): 256-268.

Hardy, R.L., 1971. Multiquadric equations of topography and other irregular surfaces. Journal of geophysical research, 76(8): 1905-1915.

Karimi, P., Bastiaanssen, W.G., 2015. Spatial evapotranspiration, rainfall and land use data in water accounting–Part 1: Review of the accuracy of the remote sensing data. Hydrology and Earth System Sciences, 19(1): 507-532.

Kobold, M., Sušelj, K., 2005. Precipitation forecasts and their uncertainty as input into hydrological models. Hydrology and Earth System Sciences, 9(4): 322-332.

Leander, R., Buishand, T.A., van den Hurk, B.J., de Wit, M.J., 2008. Estimated changes in flood quantiles of the river Meuse from resampling of regional climate model output. Journal of Hydrology, 351(3-4): 331-343.

Li, J., Heap, A.D., 2011. A review of comparative studies of spatial interpolation methods in environmental sciences: Performance and impact factors. Ecological Informatics, 6(3-4): 228-241.

Ly, S., Charles, C., Degre, A., 2011. Geostatistical interpolation of daily rainfall at catchment scale: the use of several variogram models in the Ourthe and Ambleve catchments, Belgium. Hydrology and Earth System Sciences, 15(7): 2259-2274.

Ly, S., Charles, C., Degré, A., 2013. Different methods for spatial interpolation of rainfall data for operational hydrology and hydrological modeling at watershed scale: a review. Biotechnologie, Agronomie, Société et Environnement, 17(2): 392-406.

Maggioni, V., Meyers, P.C., Robinson, M.D., 2016. A review of merged high-resolution satellite precipitation product accuracy during the Tropical Rainfall Measuring Mission (TRMM) era. Journal of Hydrometeorology, 17(4): 1101-1117.

Marshall, J.S., Palmer, W.M.K., 1948. The distribution of raindrops with size. Journal of meteorology, 5(4): 165-166.

Moulin, L., Gaume, E., Obled, C., 2009. Uncertainties on mean areal precipitation: assessment and impact on streamflow simulations. Hydrology and Earth System Sciences Discussions, 13(2): 99-114.

Neary, V., Habib, E., Fleming, M., 2004. Hydrologic modeling with NEXRAD precipitation in middle Tennessee. Journal of Hydrologic Engineering, 9(5): 339-349.

Ochoa-Rodriguez, S., Wang, L.P., Willems, P., Onof, C., 2019. A review of radar-rain gauge data merging methods and their potential for urban hydrological applications. Water Resources Research, 55(8): 6356-6391.

Oke, A., Frost, A., Beesley, C., 2009. The use of TRMM satellite data as a predictor in the spatial interpolation of daily precipitation over Australia, Proceedings of the 18th World IMACS/MODSIM Congress.

Otieno, H., Yang, J., Liu, W., Han, D., 2014. Influence of rain gauge density on interpolation method selection. Journal of Hydrologic Engineering, 19(11): 04014024.

Pebesma, E.J., Wesseling, C.G., 1998. Gstat: a program for geostatistical modelling, prediction and simulation. Computers & Geosciences, 24(1): 17-31.

Pegram, G., 2001. Spatial interpolation and mapping of rainfall: 3. Optimal integration of rain gauge, radar & satellite-derived data in the production of daily rainfall maps. Progress Report to the Water Research Commission, for the Period April.

Price, D.T., McKenney, D.W., Nalder, I.A., Hutchinson, M.F., Kesteven, J.L., 2000. A comparison of two statistical methods for spatial interpolation of Canadian monthly mean climate data. Agricultural and Forest meteorology, 101(2-3): 81-94.

Ryzhkov, A.V., Giangrande, S.E., Schuur, T.J., 2005. Rainfall estimation with a polarimetric prototype of WSR-88D. Journal of Applied Meteorology, 44(4): 502-515.

Schuurmans, J., Bierkens, M., 2006. Effect of spatial distribution of daily rainfall on interior catchment response of a distributed hydrological model. Hydrology and Earth System Sciences Discussions, 3(4): 2175-2208.

Shaw, E.M., Lynn, P., 1972. Areal rainfall evaluation using two surface fitting techniques. Hydrological Sciences Journal, 17(4): 419-433.

Sinclair, S., Pegram, G., 2005. Combining radar and rain gauge rainfall estimates using conditional merging. Atmospheric Science Letters, 6(1): 19-22.

Singh, V., 1997. Effect of spatial and temporal variability in rainfall and watershed characteristics on stream flow hydrograph. Hydrological processes, 11(12): 1649-1669.

Smith, J.A., Baeck, M.L., Meierdiercks, K.L., Miller, A.J., Krajewski, W.F., 2007. Radar rainfall estimation for flash flood forecasting in small urban watersheds. Advances in Water Resources, 30(10): 2087-2097.

Teegavarapu, R.S., Tufail, M., Ormsbee, L., 2009. Optimal functional forms for estimation of missing precipitation data. Journal of hydrology, 374(1-2): 106-115.

Tetzlaff, D., Uhlenbrook, U., 2005. Effects of spatial variability of precipitation for process-orientated hydrological modelling: results from two nested catchments. Hydrology and Earth System Sciences Discussions, 2(1): 119-154.

Thiessen, A.H., 1911. Precipitation averages for large areas. Monthly weather review, 39(7): 1082-1089.

Thorndahl, S. et al., 2017. Weather radar rainfall data in urban hydrology. Hydrology and Earth System Sciences, 21(3): 1359-1380.

Vicente-Serrano, S.M., Saz-Sánchez, M.A., Cuadrat, J.M., 2003. Comparative analysis of interpolation methods in the middle Ebro Valley (Spain): application to annual precipitation and temperature. Climate research, 24(2): 161-180.

Wackernagel, H., Oliveira, V.D., Kedem, B., 1997. Multivariate geostatistics. SIAM Review, 39(2): 340-340.

Wagner, P.D., Fiener, P., Wilken, F., Kumar, S., Schneider, K., 2012. Comparison and evaluation of spatial interpolation schemes for daily rainfall in data scarce regions. Journal of Hydrology, 464: 388-400.

Zimmerman, D., Pavlik, C., Ruggles, A., Armstrong, M.P., 1999. An experimental comparison of ordinary and universal kriging and inverse distance weighting. Mathematical Geology, 31(4): 375-390.

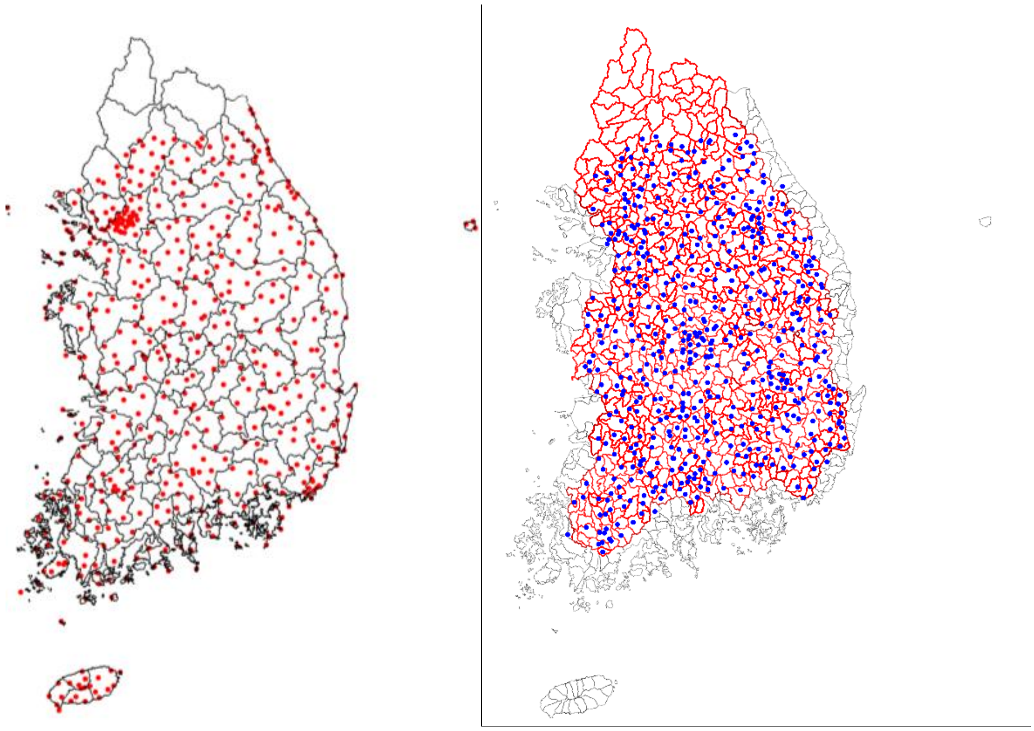

(a) Sub-basins and KMA rain gauges (b) Standard-basins and ME rain gauges

Figure 1. (a) 117 Medium sized Sub-basins (black polygons) and Automatic Weather Stations (AWS) of the Korea Meteorological Administration (KMA) (left red dots) for water management. (b) 850 Small sized Standard-basins for flood forecasting. Red polygons (664 Standard-basins) represent the basins which are used in river flood forecasting and blue dots are rain gauges installed by Ministry of Environment (ME).

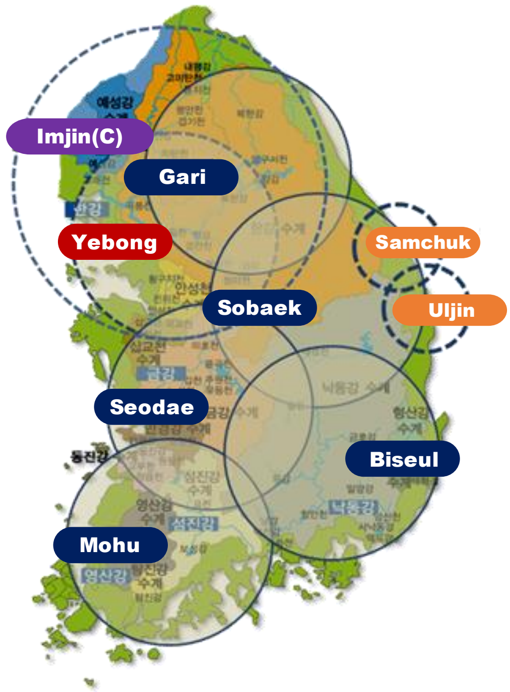


Figure 2. Locations and observation ranges of ME weather radars. Gari, Yebong, Sobaek, Seodae, Mohu, Biseul are S-band dual-polarization radars, Imjin(C) is a C-band single-polarization radar, and Samchuk, Uljin are small X-band radars for gap-filling large S-band radar networks.

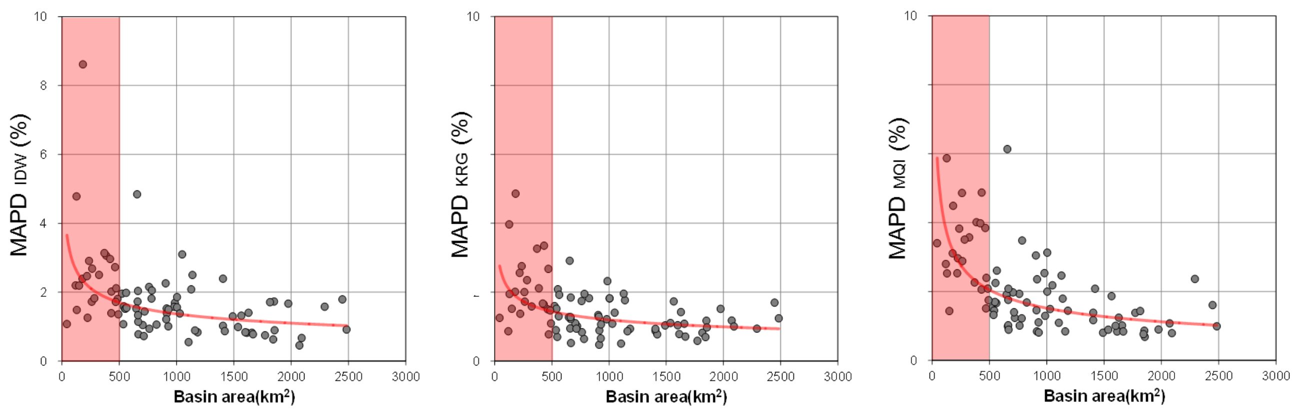


Figure 3. Mean absolute percentage discrepancy (MAPD) of areal mean annual rainfall for different spatial interpolation schemes and catchment areas. IDW, KRG and MQI represent Inverse Distance Weighting, Kriging and Multiquadric Interpolation respectively. The pink shading covers the smaller areas.

.

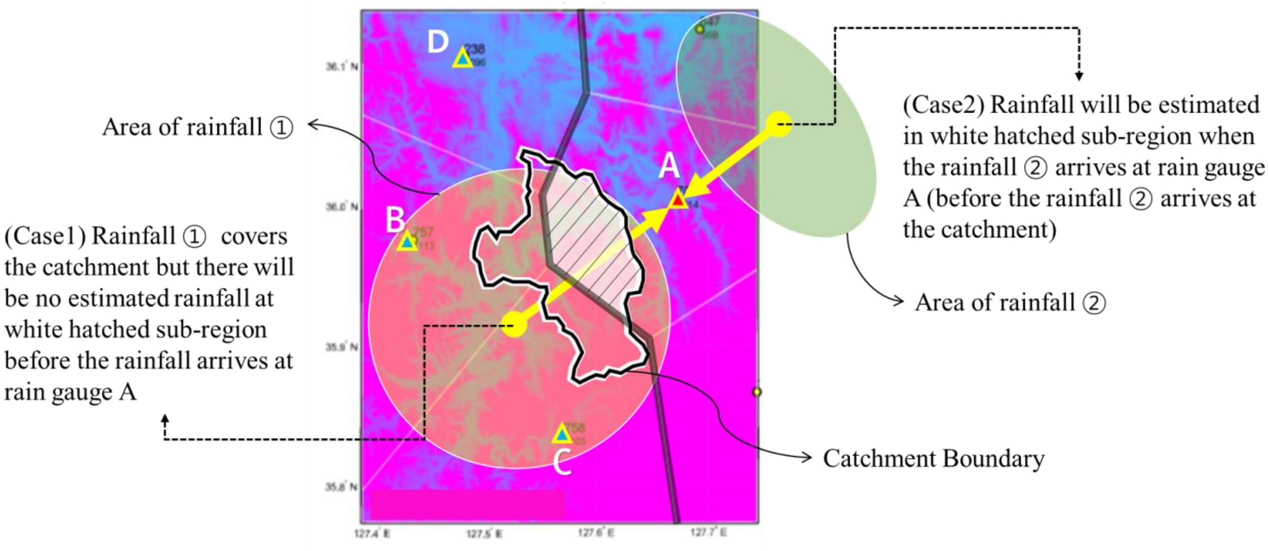


Figure 4. Illustration of the drawback of the Thiessen polygon method (TSN). An example of four rain gauges (A, B, C, D) located outside the catchment and the storm moving from South West to North East (Case 1) and vice versa (Case 2).

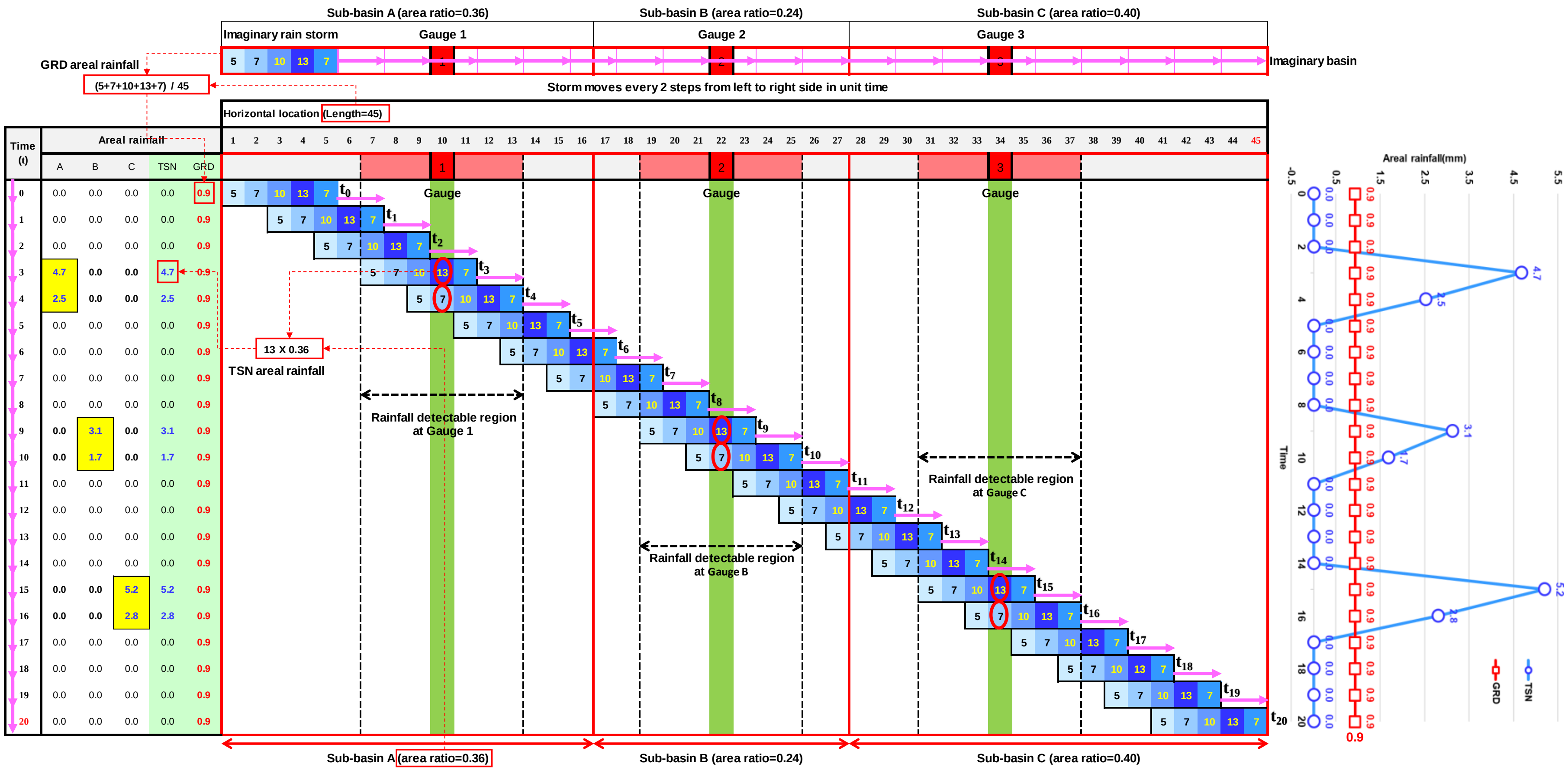


Figure 5. Schematic example of rainfall movement and Thiessen polygon (TSN) method. This figure is an example showing the characteristics of precipitation calculated by the TSN when the distance between rain gauges are set further apart than the storm size. The example consists of hypothetical rainfall (rainfall distribution 5, 7, 10, 13, 7mm), three catchments (Sub-basin A, B, C) and three rain gauges (Gauge 1, 2, 3). The horizontal axis represents distance and the vertical axis represents time. Here, the units of time and distance are ignored because it is a hypothetical example. The figure represents that the imaginary rainfall at the top shifts by 2 steps in a unit time from 0 to 20 time steps. Red boxs 1, 2, and 3 indicate rainfall gauges, respectively. The line graph on the right panel shows areal mean rainfall over time calculated by the TSN method and the grid mean rainfall (GRD) method. The GRD is constant over time, while TSN is fluctuating sharply.

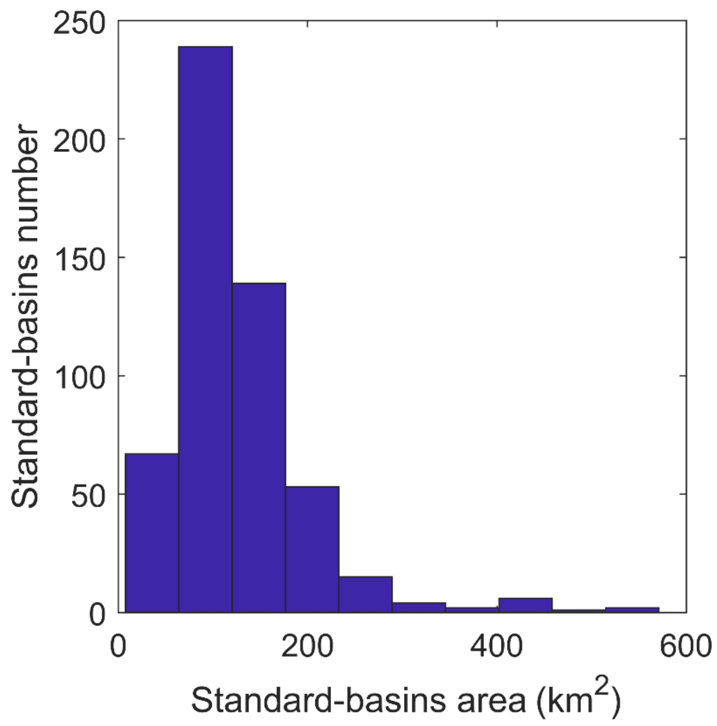


Figure 6. Areal distribution of 528 standard-basins. The mean value of 528 standard-basins area is 126 km$^2$.

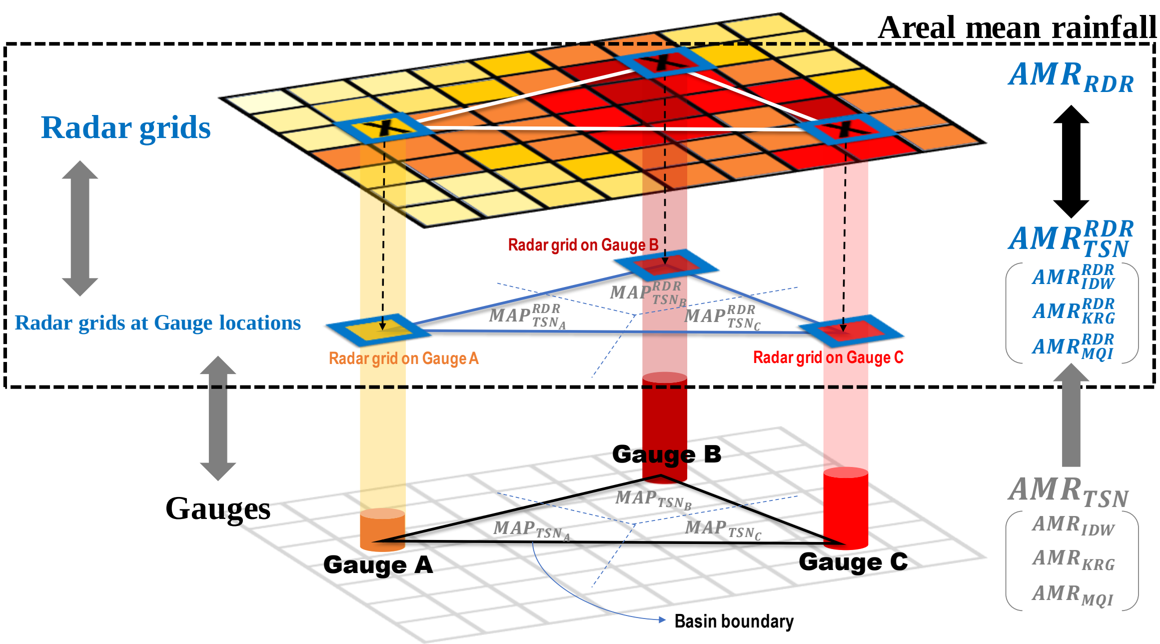


Figure 7. Schematic illustration of estimating areal mean rainfall with different interpolation methods using radar rainfall data. TSN, IDW, KRG and MQI are interpolation methods respectively. $AMR^{RDR}_{GRD}$ is areal mean rainfall estimated from radar grid rainfall.

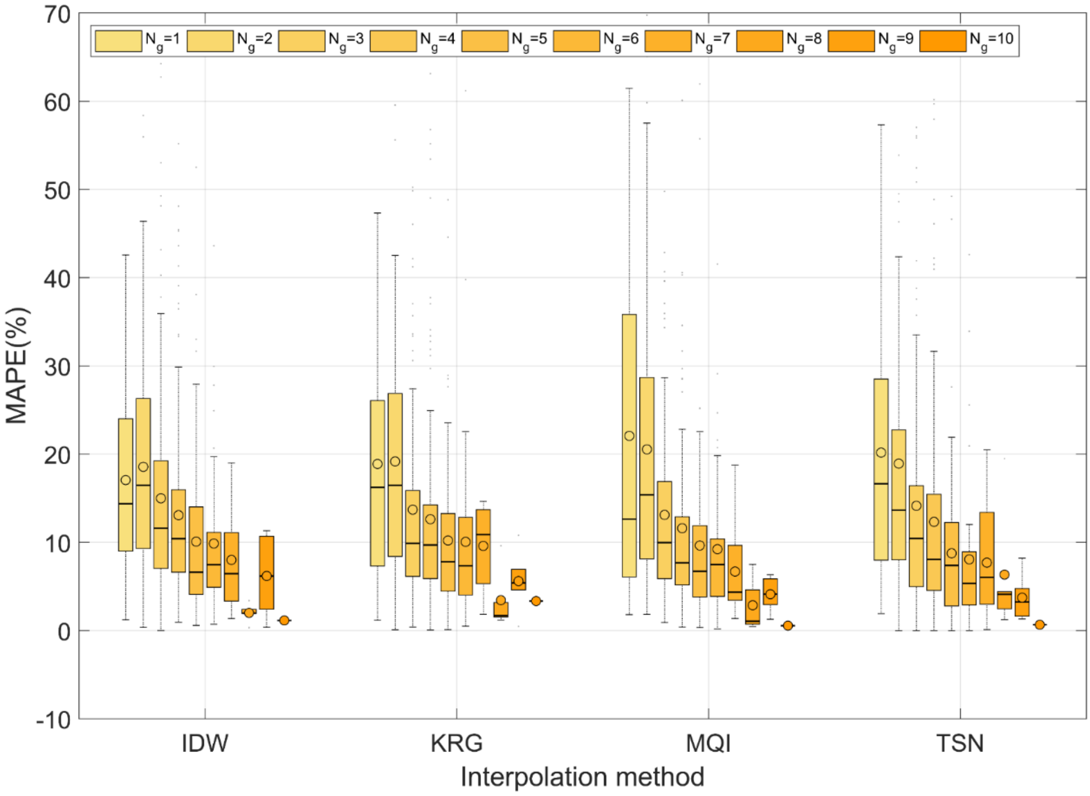


Figure 8. Boxplots of mean absolute percentage error (MAPE, %) with respect to different number of rain gauges ($N_g$) and different spatial interpolation methods. The horizontal line in the box represents the median value and the black circle represents the mean value. The box height represents the 25th percentile (1st quartile) to the 75th percentile (3rd quartile) of MAPE sets.The whiskers are the two lines outside the box that extend to the highest and lowest values. IDW, KRG, MQI and TSN represent Inverse Distance Weighting, Kriging, Multiquadric Interpolation and Thiessen polygon respectively.

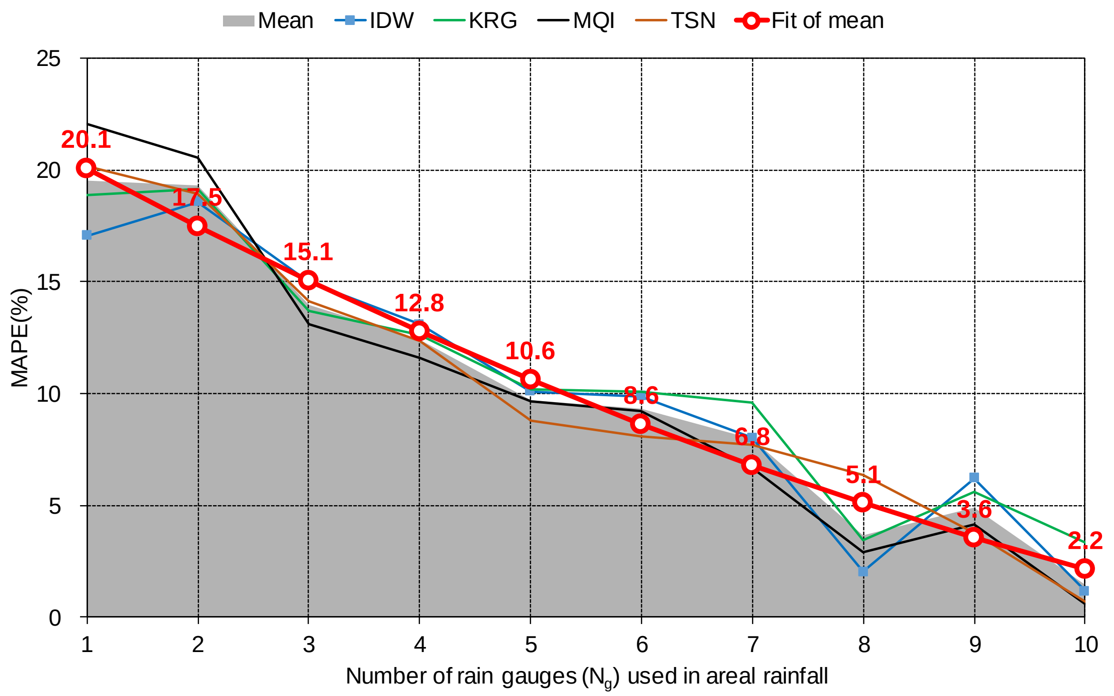


Figure 9. Mean value of MAPE (%) with respect to each number of rain gauges ($N_g$) in Figure 8. MAPE decreases for all interpolation methods as number of rain gauges increase.

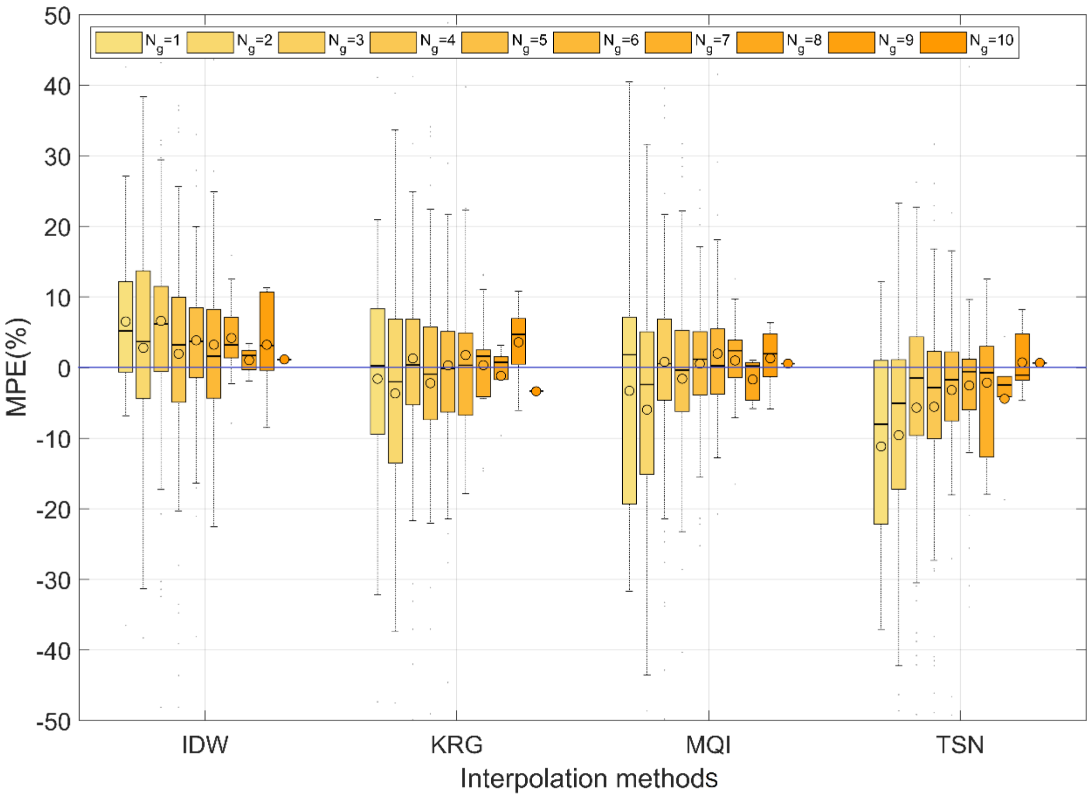


Figure 10. Boxplots of Mean percentage error (MPE, %) with respect to different number of rain gauges ($N_g$) and different spatial interpolation methods. The horizontal line in the box represents the median value and the black circle represents the mean value. The box height represents the 25th percentile (1st quartile) to the 75th percentile (3rd quartile) of MPE sets. The whiskers are the two lines outside the box that extend to the highest and lowest values. IDW, KRG, MQI and TSN represent Inverse Distance Weighting, Kriging, Multiquadric Interpolation and Thiessen polygon respectively.

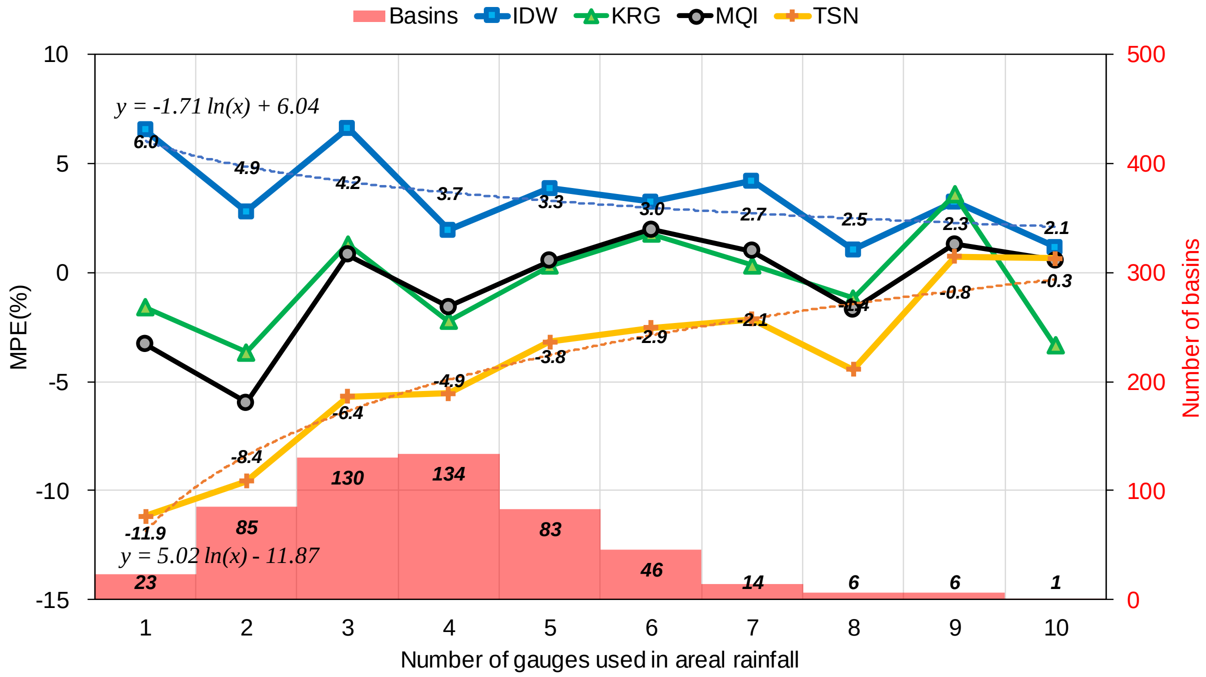


Figure 11. Mean value of MPE is extracted from Figure 10. Yellow line show MPE of TSN with respect to $N_g$, blue line show MPE of IDW, green line show MPE of KRG and black line show MPE of MQI. Red histogram shows the number of standard-basins. Blue dotted line is the fitted curve of MPE of IDW and yellow dotted line is the fitted curve of MPE of TSN.

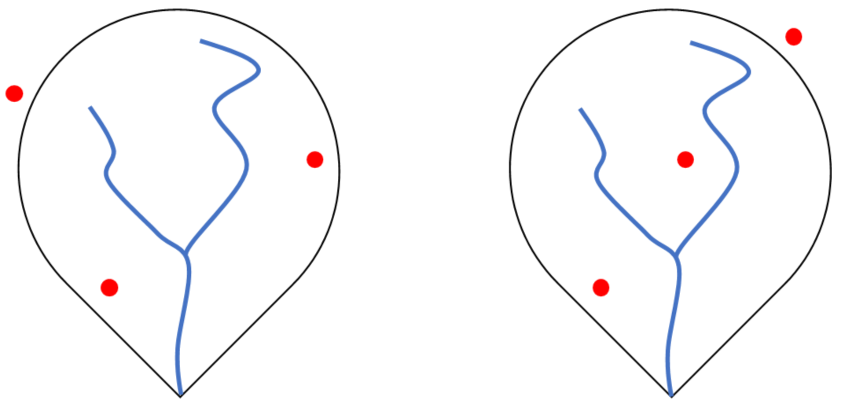

(a) radially located rain gauges (b) linearly located rain gauges

Figure 12. Schematic of rain gauge distribution. Black line is the boundary of hypothetic basin and red dots are rain gauges.

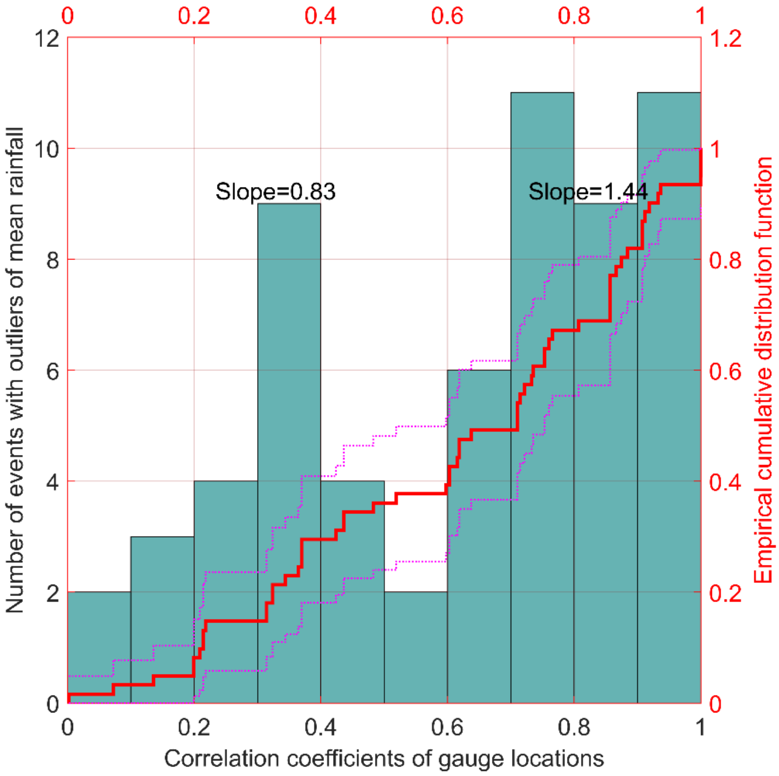


Figure 13. Relationship between number of areal mean rainfall outliers in 61 rainfall events and correlation coefficients of rain gauge geographic locations based on latitude and longitude in 664 Standard-basins. The solid red line represents the empirical cumulative distribution function (ECDF, right y-axis) of this bar graph series, and the pink dotted lines represent the 95% confidence interval of ECDF. The slope of outlier occurrence changes from 0.83 to 1.44 before and after when the correlation coefficient is 0.7.

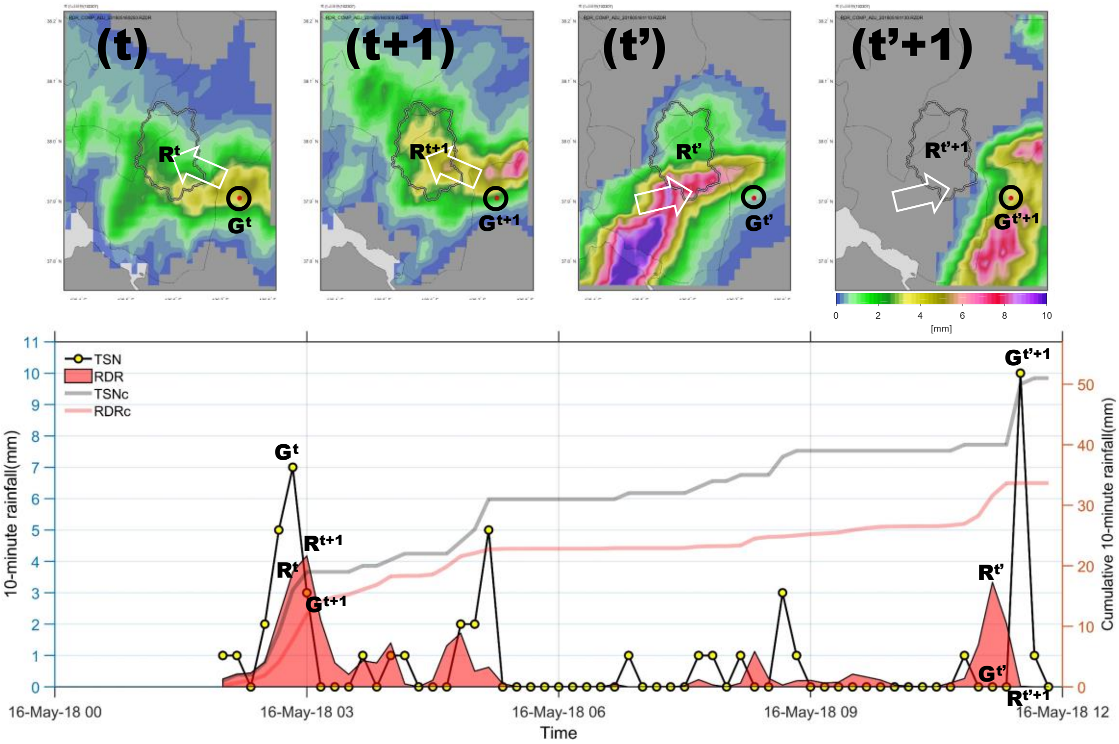


Figure 14. An example showing the time lag of peak rainfall occurrence depending on the distribution of rain gauges and rainfall movement on 15 May, 2018. The rain gauge is located outside the catchment on the bottom right of the 4 colored maps (black circle in the upper panel). In the beginning of the rainfall event (time $t$ and $t + 1$, the sampling time interval is 10-minutes), the storm is moving from right to left , as shown in the first two of the 4 panels above the time series, but changes direction about 9 hours later. The time-shift in the two periods are lagged by distance as can be seen the lower panel.. The white arrows indicate the direction of rainfall movement. TSN and RDR represent the areal rainfall using the Thiessen polygon method and radar areal mean rainfall, respectively. TSNc and RDRc represent the cumulative areal rainfall using the Thiessen polygon method and cumulative radar areal mean rainfall over the catchment, outlined in grey in the upper 4 panels, respectively.